Personalizing Cardiovascular Simulations for Wearable Health Sensing

Tommy DeBenedetti, Parker Ruth, James Landay

Stanford University Human Computer Interaction Group

INTRODUCTION

Cardiovascular disease is the leading cause of death in the United States [1] and globally, accounting for 20.5 million deaths in 2021 (approximately ⅓ of all deaths that year) [2]. However, with intervention, many cardiovascular diseases are reversible [3], [4], [5]; therefore, it is crucial to have excellent diagnostic tools.

One particularly pervasive risk factor for cardiovascular disease is hypertension, or high blood pressure [5]. Thus, precisely measuring blood pressure is crucial for promoting cardiovascular health. While existing tools like brachial cuffs are adequate for in-clinic measurements, they cannot capture continuous blood pressure data over time. More generally, tools for measuring the continuous dynamics of the cardiovascular system remain extremely limited.

Wearable technology may provide a pathway to more continuous sensing. Wearable sensors are limited to parts of the body that people find acceptable for long-term use—in particular, the wide adoption of smartwatches shows that the wrist is one such spot. This poses a challenge since many key cardiovascular metrics are localized near the heart. For example, blood pressure is most predictive of cardiovascular health when measured near the heart [6]. We propose that data from a wrist-worn wearable device might be able to serve as a "fingerprint" of a person's cardiovascular system, from which we could construct a personalized "digital twin."

A digital twin is a computational cardiovascular model personalized to an individual's physiology. The cardiovascular system can be modeled with different levels of fidelity, ranging from from 3D to 0D. We focus on 0D lumped parameter models for the sake of their computational efficiency [7], [8]. In a 0D cardiovascular model, each blood vessel is represented with a resistor (R), inductor (L), and capacitor (C) [8]; a unique configuration of these parameters define a patient's digital twin.

The challenge in achieving these digital twins is in fitting all of a model's parameters to data collected at a single point on the body. This raises the following questions: Can wearable sensor data uniquely determine a full cardiovascular model? If not a full cardiovascular model, could a model with fewer parameters more likely be uniquely determined? Can models with fewer parameters reproduce the behavior of more complex models? How do we fit those parameters from the infinite possibilities? How do we search that space when we have no closed form loss function for gradient descent?

This work aims to answer these questions. First, we investigate methods for reducing 0D model complexity while preserving the crucial properties for blood pressure detection. Second, we experiment with a probabilistic algorithm for fitting 0D models to wearable-collected data.

While digital twins have the potential for broad applications to various cardiovascular diagnoses, this research focuses particularly on blood pressure because it has a well established need. We will return periodically to central blood pressure estimation from a wrist-based sensor as a motivating example.

Model Reduction

MODEL REDUCTION METHODS

A 0D model is defined by an aortic root inflow, the RLC values of each vessel, the connections between vessels, and lumped parameter boundary conditions which simplify downstream vasculature [8]. We simulate 0D models using either Spice [9] for AC analysis or SimVascular [8] for transient analysis. The following methods of model reduction are all performed and evaluated on one 0D "patient," specifically a synthetic patient from the 1D dataset [10] constructed by Charlton et al. which was previously converted into an equivalent 0D form. Charlton's model consists of 116 vessels [10], so in 0D form it has 448 parameters, as visualized in Figure 0.

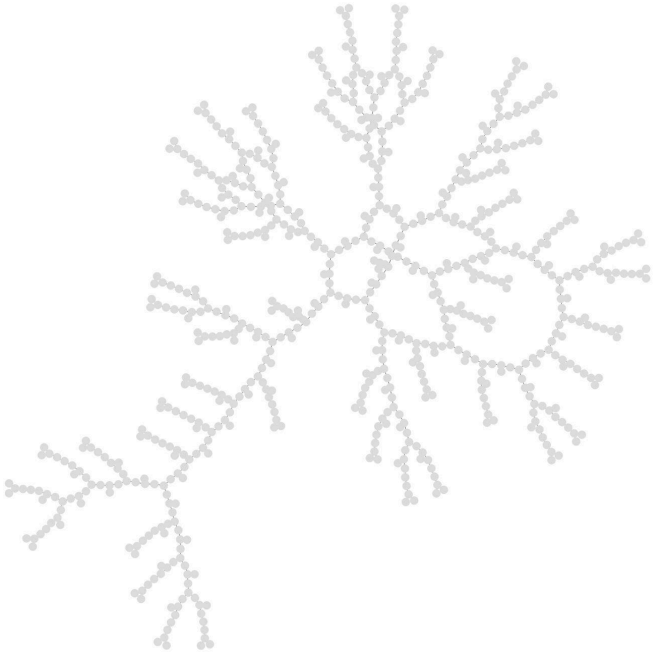

Figure 0: A graph representation of a 116-vessel 0D model of the cardiovascular system in which each node represents a junction or a circuit component comprising either a boundary condition or a blood vessel.

In order to make our model more feasible for simulating and fitting, we set out to simplify the model while preserving its most important behavior. What behavior we consider the most important and how we evaluate it are application specific; here, we consider our guiding application of estimating aortic blood pressure from wrist-worn sensors. We quantify how similarly two models behave by comparing the transfer function between the aortic and radial pressures. The aortic-to-radial transfer function characterizes the relationship between the data we can sense and the data we wish to estimate. Specifically, we compare these transfer functions on the frequency range 0Hz-100Hz. While pulse waves typically consist mostly of lower frequencies [11], our goal in model reduction is to theoretically reproduce the behavior of the full model as exactly as possible.

We explored two methods for producing reduced-complexity models: a top down-method and a bottom-up method.

Top-Down Model Reduction

In the top-down method, model reduction was performed by sequentially removing vessels that minimized the model's error. Model error was measured by root mean squared error of the transfer function magnitude. We hypothesized that a greedy algorithm might fail because it assumes that for any $n > m$, the best m vessels to remove are necessarily a subset of the best n vessels to remove. Instead, we use a beam search algorithm. Starting with the full model, the beam search keeps, at each step, the n best thus-far-reduced models; for each step, it considers removing each remaining vessel from each of the stored models and keeps the n best of the resultant, further reduced models. The data presented here uses a beam search with width n=10.

At each iteration, vessels are removed by deleting the RLC vessel unit and connecting the vessel's input to its output. In some cases this can lead to zero-impedance loops, which have an undefined current, and therefore make the matrix formulation that Spice uses to simulate circuits not uniquely solvable. We avoid this by always adding a very small resistor in place of the vessel.

Bottom Up Model Reduction

As an alternative to the top-down model reduction strategy, we explored a bottom-up approach. Incorporating domain knowledge of important elements of cardiovascular structure and experience with reduced 0D models, we designed custom cardiovascular models. Defining a cardiovascular model consists of defining which vessels are included, their parameters, how they are connected, the system's inflow from the heart, and its boundary conditions. The structure of our models was constructed by trial and error—guided by the goal of making a minimal structure while retaining all of the system's high level structure. The inflow was adopted from the one 0D

simulation defined previously, to mimic a physiologically realistic blood flow. The boundary conditions were copied from those in the analogous region of the original 116-element model.

Vessels in these bottom-up-produced models do not directly correspond to any individual vessels in the full model, which creates ambiguity in choosing their parameters. To determine appropriate parameters, we used the SimVascularZeroDCalibrator, which fits a 0D model's RLC parameters to reproduce data about the blood flow at the input and output of each vessel [8]. Since the vessels of the reduced model do not have a direct correspondence to those in the 116-vessel model, we must somehow map the blood flow data we do have for a 116-vessel model into the reduced model. We apply hemodynamic heuristics to perform this mapping, which Figure 1 illustrates.

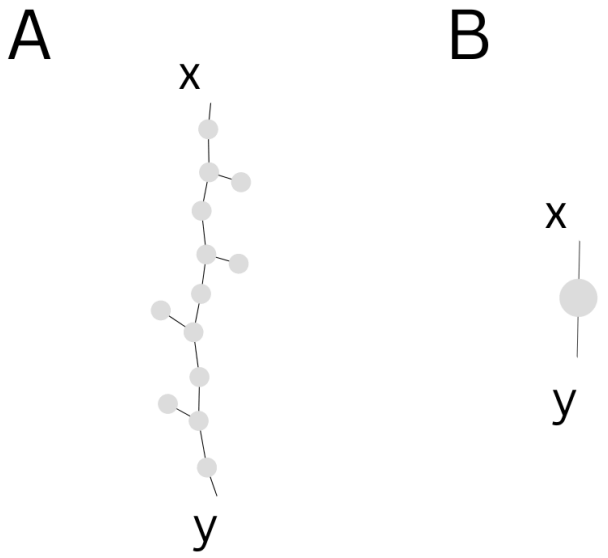

Figure 1: Graphs, in which a node represents a vessel, representing the same region in two models. To convert the vascular structure in A to the single vessel in B, let the blood flow at the identified points of B be equal to the corresponding parts in A.

MODEL REDUCTION RESULTS

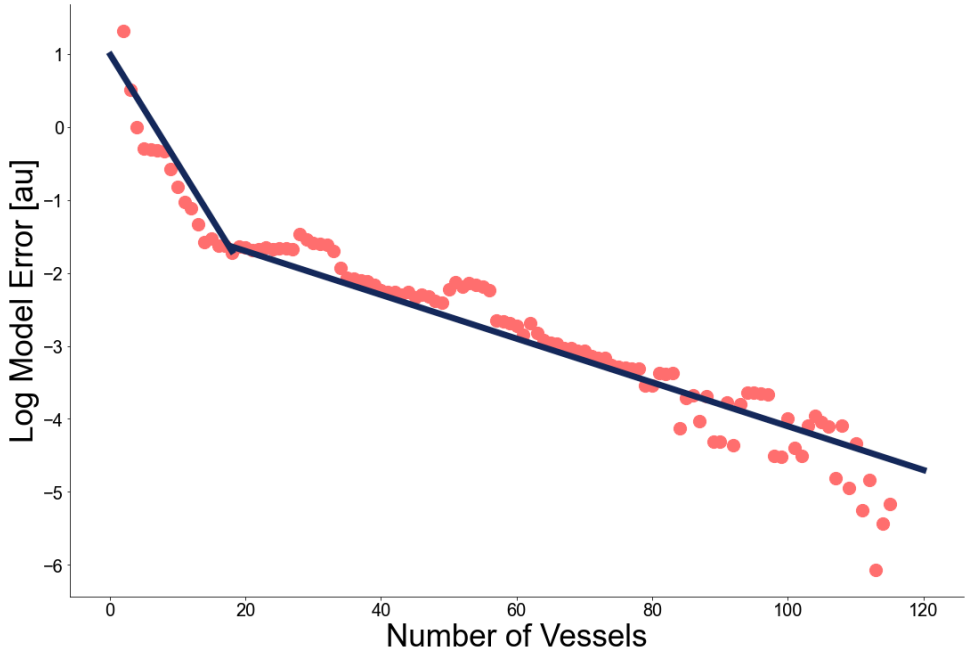

Figure 2: The effectiveness of the best top-down-produced model and approximate trend lines showing an inflection in the rate of error decline at around 20 vessels. The y-axis is the base-10 log of the RMSE between the original 116-vessel model's gain magnitude and the top-down-produced model's.

From Figure 2, we identify 20 vessels as a target model size because, at that point, the rate at which increasing model size improves model fidelity decreases. So, we created 20 vessel models with each of the described model reduction methods, which are shown in Figure 3.

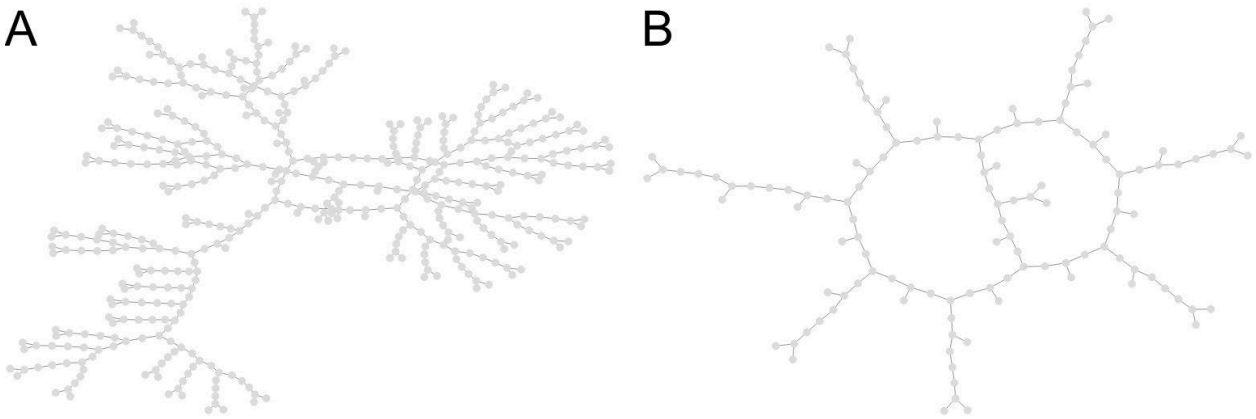

Figure 3: Graphs of 20-vessel models produced through the top-down method (A) and the bottom-up method (B). Note that A has more nodes because of the small resistor added for each vessel removed.

As seen in Figure 4, the top-down approach outperforms the bottom-up approach—quantitatively, the RMSEs of their gain magnitudes with that of the original model are 720 and 2150 respectively.

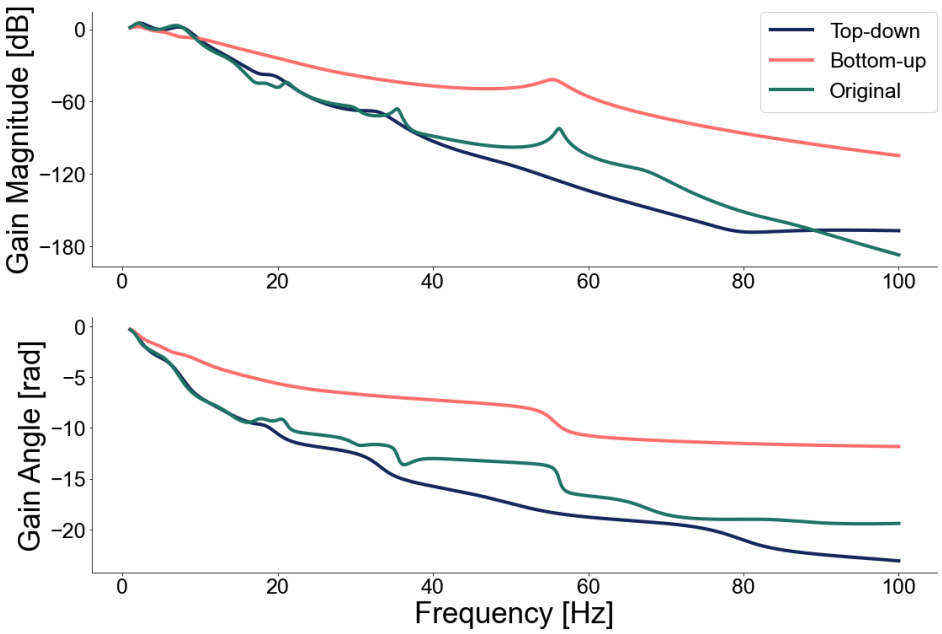

Figure 4: The transfer functions of 20 vessel models produced by each method compared to the original.

Figure 4 shows that while both methods seem capable of retaining the general shapes of the transfer functions, the top-down approach is more successful at capturing their magnitude and details. Furthermore, for practical purposes, the top-down approach particularly excels for lower frequencies, which may be more valuable for predicting cardiovascular health.

Model Fitting

MODEL FITTING METHODS

To fit a model to a patient, we propose an algorithm, outlined in Figure 5, which accepts as input a function describing aortic inflow and a radial pressure pulse wave and outputs a probability distribution over parameter configurations. While this algorithm is easily adaptable to various model structures, the following data and analysis arise from use on a bottom-up-produced 20 vessel model.

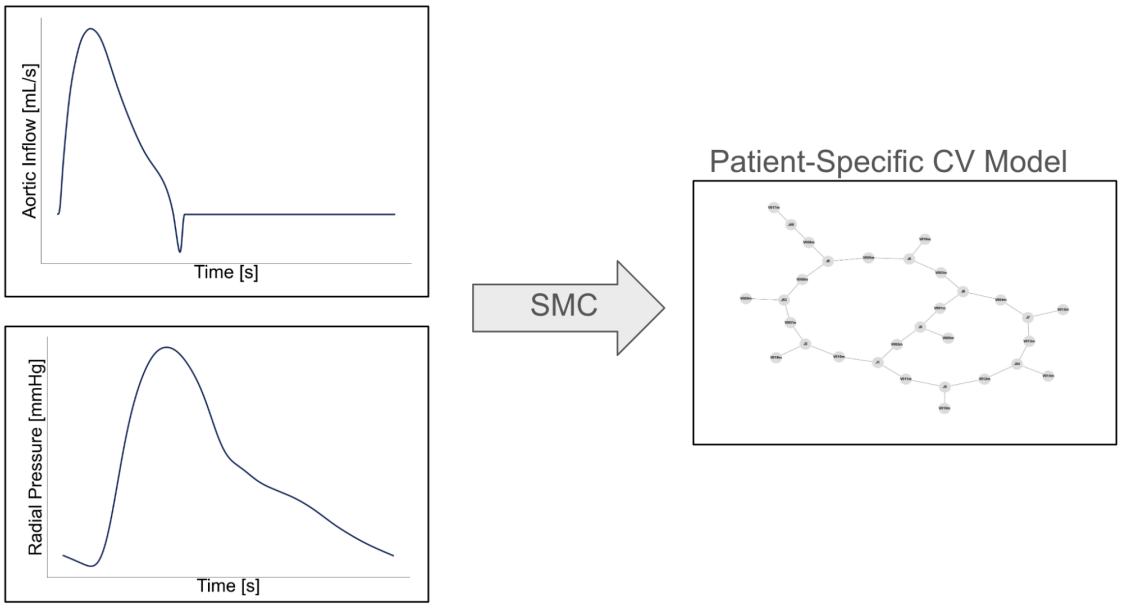

Figure 5: A flow chart depicting the outline of our algorithm. It takes two inputs—the system's inflow from the aorta and the radial pressure pulse wave—and produces as output the parameters of a patient-specific cardiovascular model through a SMC.

Our model-fitting algorithm is an adaptation of Sequential Monte Carlo (SMC), depicted conceptually in Figure 6. The 0D model's numerical simulations preclude the possibility of gradient descent with any closed form loss function. SMC overcomes this challenge by using randomness. Furthermore, in scenarios where multiple parameter configurations can similarly reproduce the radial pressure pulse wave, SMC provides the benefit of producing a sampled posterior distribution over parameter configurations rather than a single optimal solution.

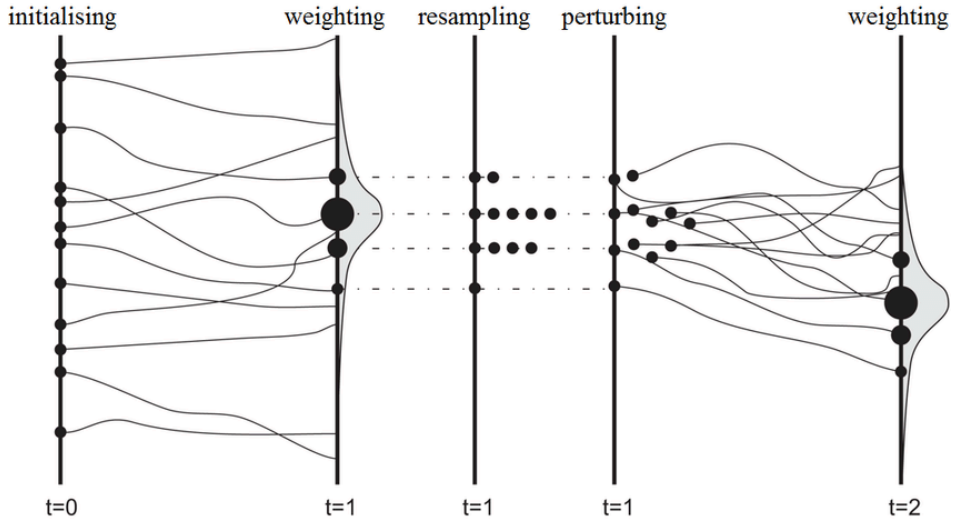

Figure 6: One iteration of general Sequential Monte Carlo for searching a 1 dimensional space. (From [12])

Assuming all 116 vessels of a full 0D model are identically distributed, we naively approximate the mean and covariance matrix of a multivariate normal distribution for the parameters of any vessel. The SMC algorithm is initialized by sampling each blood vessel from this same multivariate normal distribution. To weight a sampled particle, the model's parameters are set according to that particle, it is simulated with the provided inflow, and the inverse of the mean squared error of the transient output and the target pulse wave is assigned as the weight. Lastly, a particle is perturbed by sampling each vessel in the model from a multivariate normal update distribution. The update distribution is centered at this current particle's state with the same covariance matrix as the original initialization distribution scaled down by its weight.

MODEL FITTING RESULTS

We ran the model fitting algorithm with 100 particles and 50 iterations. Figure 7 demonstrates that a reduced model can successfully be fit to reproduce a radial pulse wave. The model's radial pressure pulse wave's root mean squared error with the target pulse wave decreases from 21,000 initially to 5,600 after 10 SMC iterations to 1,400 after 50 SMC iterations.

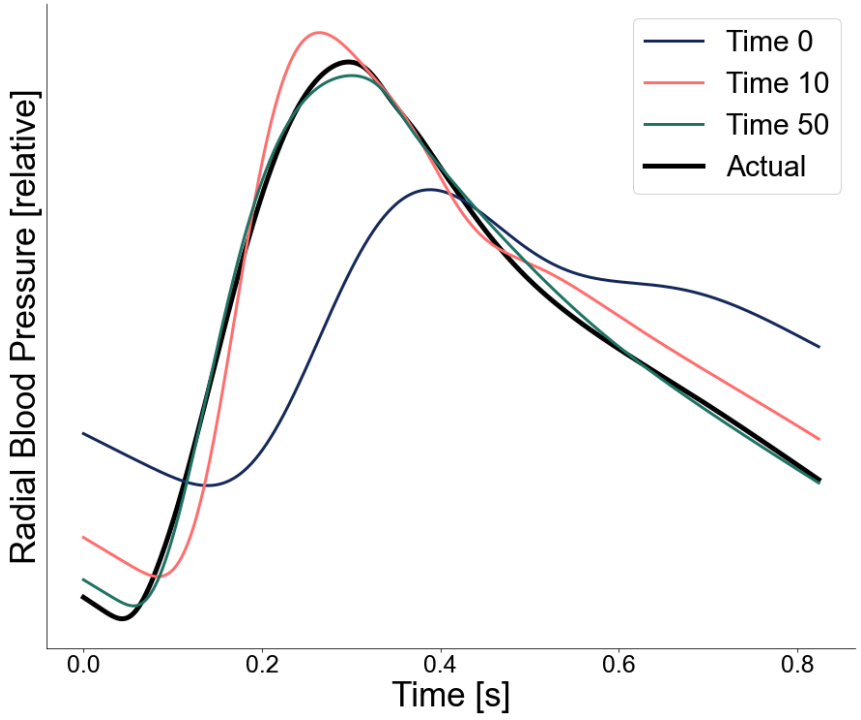

Figure 7: The target radial pulse wave for one run of the model fitting algorithm and the radial pulse wave produced by the best particle after various numbers of iterations of SMC.

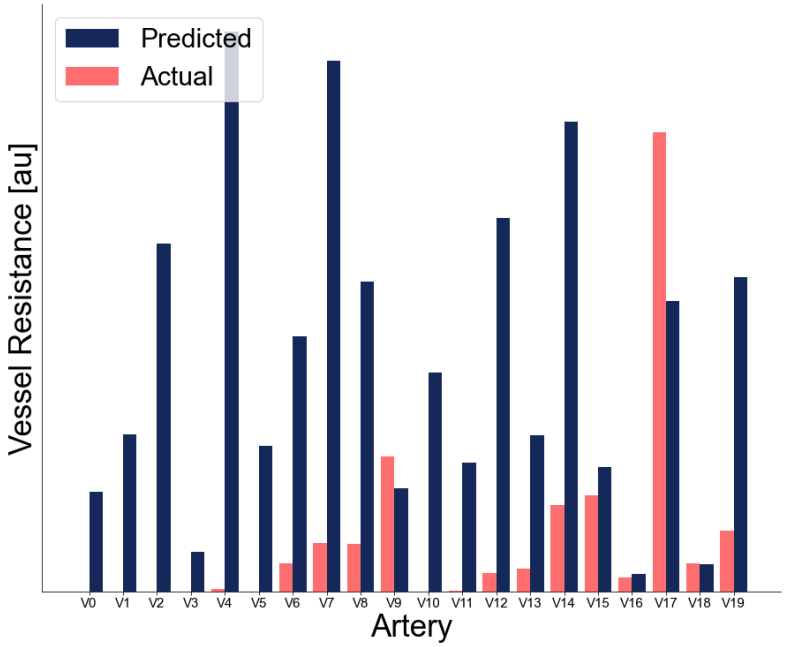

Figure 8: The resistance values fit for each vessel for a particular radial pulse wave and the actual resistances which produced that pulse wave.

As seen in Figure 8, the parameters fit by SMC do not match the actual parameters used to produce the target pulse wave. The algorithm cannot distinguish between multiple parameter configurations which produce similar, or even identical, radial pressure pulse waves. In fact, some predictions are wrong by multiple orders of magnitude; for the vessel labeled V0 in Figure 8, which corresponds to the aorta, the largest artery in the body [10], the predicted resistance is 43,000x the actual value.

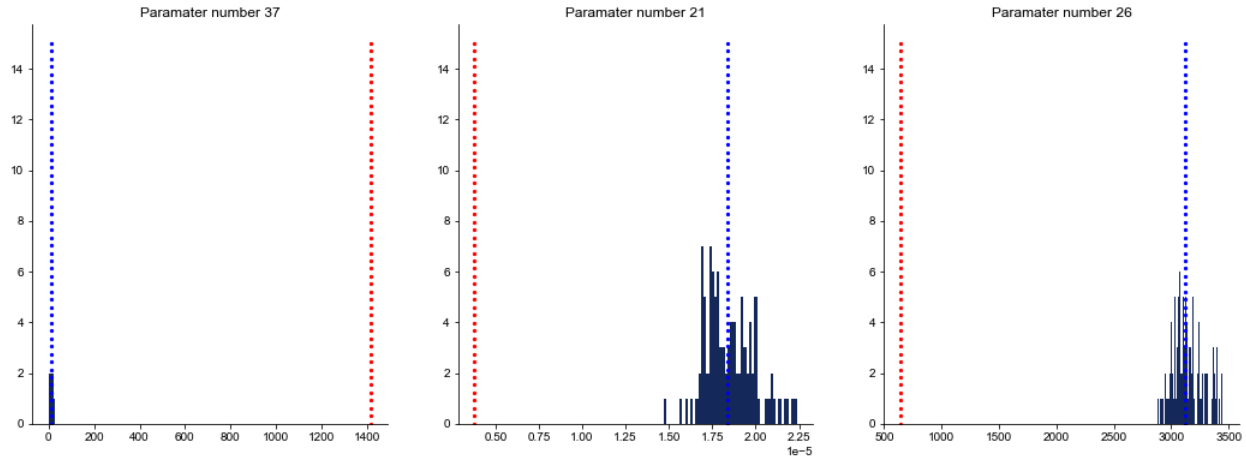

Figure 9: The distribution of (from left to right) the inductance of Vessel 12, the capacitance of Vessel 7, and the resistance of Vessel 8 for all 100 particles after 50 iterations of SMC. The blue dotted lines represent the expectation of each distribution, and the red dotted lines represent the actual value of each parameter.

Notably, Figure 9 shows that the algorithm does converge on a sampled posterior distribution; however, the R, L, and C values all disagree by orders of magnitude from the target values.

DISCUSSION

Interpretation

A particularly interesting result is the stark difference in performance between the two methods for model-reduction. We speculate this may be in part due to the process with which we mapped blood flow for calibration of bottom-up models (Figure 1), which violates conservation laws because it disregards all of the blood that flows out of the offshoots of the structure in A. While the calibrator has methods built in to resolve these violations, they may have resulted in unexpected behavior of the circuit.

In the model fitting process, we were surprised to observe fitted solutions that successfully reproduced the radial artery pulse wave while using starkly different parameters than the original, including at the radial artery itself. In Figure 8, V0 and V6 represent the aorta and radial artery respectively; even here, the predicted resistance for the radial artery was approximately 10 times the actual.

Given the high dimensionality of the parameter space, it is unsurprising that there might be multiple parameter configurations which produce the same radial output. However, it was surprising that our SMC algorithm converged to a distribution with a single *incorrect* mode rather than representing a multimodal posterior distribution. It could be that there were not enough particles to cover the search space or that our naive prior distribution put such low density on physiologically realistic configurations that true solutions were extremely unlikely to be represented in the posterior.

Future Work

Although it was less successful here than the top-down approach, the bottom-up method for model simplification should be refined rather than discarded. The current model uses arbitrary boundary conditions. Experimentation with these boundary conditions or modification of the calibration tool such that it can also calibrate boundary condition values may significantly improve bottom-up model performance. Improvement to the top-down model reduction method should incorporate re-calibration after each vessel removal and should resolve issues with zero impedance loops with more precision by adding small resistance only when needed or otherwise removing loops as they arise. Furthermore, when calibrating reduced 0D models produced by either method, the process by which full model blood flow is mapped to reduced models can be

improved. Alternate heuristics to apply in this process are ensuring that the inflow and outflow of each vessel in the reduced model are equal or forcing that the proportions of each junction's inflows and outflows be preserved in reduction.

Further work should also improve the model fitting algorithm by incorporating metrics other than pressure measured at the wrist (for example, flow rate or arterial area). Additionally, the prior distribution over parameter configurations can be improved to encode the knowledge that different arteries' anatomical and physiological variables are distributed differently. Lastly, in order to make digital twins realizable with purely wearable technology, the algorithm must be reconfigured so as not to require an aortic inflow curve as input; one solution we suggest is aiming to reproduce a target aortic-to-radial transfer function rather than a target transient radial output because it also may further distinguish between parameter configurations which produce the same radial output for just the particular provided inflow.

Additionally, improving available computing resources or improving the efficiency with which we compute particle weights will enable future work to make valuable changes to hyperparameters of SMC — including the temperature of perturbation, the number of particles, and the number of iterations — which will increase the complexity of the posterior distribution.

CONCLUSION

We have demonstrated the possibility of reducing 0D models while preserving important properties — particularly, the aortic-to-radial transfer function — and established multiple methods for doing so. Furthermore, we have established working models on which model fitting can be experimented. For the challenge of model fitting, we have prototyped an SMC-based algorithm, which succeeds in fitting some parameters to reproduce a provided radial pulse wave.

The model reduction and model fitting algorithms presented here could be essential stepping stones in developing a comprehensive toolkit for personalized cardiovascular simulations. These "digital twins" would be an invaluable tool to cardiovascular health professionals, complementing their current suite of cardiovascular diagnostic tools with temporal, dynamic information about the whole cardiovascular system. By enabling more personalized and continuous assessments of cardiovascular state, this could help promote healthy hearts with accessible, wearable devices.

REFERENCES

[1] K. D. Kochanek, S. L. Murphy, J. Xu, and E. Arias, “Mortality in the United States, 2022”, Accessed: Aug. 28, 2024. [Online]. Available: https://stacks.cdc.gov/view/cdc/135850

[2] M. Di Cesare *et al.*, “The Heart of the World,” *Glob. Heart*, vol. 19, no. 1, p. 11, doi: 10.5334/gh.1288.

[3] R. Nagarakanti, D. Whellan, S. Rubin, and P. J. Mather, “Reversible cardiomyopathies,” *Cardiol. Rev.*, vol. 15, no. 4, pp. 178–183, 2007, doi: 10.1097/CRD.0b013e31804c98b1.

[4] J. E. Rame, “Chronic heart failure: a reversible metabolic syndrome?,” *Circulation*, vol. 125, no. 23, pp. 2809–2811, Jun. 2012, doi: 10.1161/CIRCULATIONAHA.112.108316.

[5] P. L. Valenzuela *et al.*, “Lifestyle interventions for the prevention and treatment of hypertension,” *Nat. Rev. Cardiol.*, vol. 18, no. 4, pp. 251–275, Apr. 2021, doi: 10.1038/s41569-020-00437-9.

[6] M. E. Safar and P. Jankowski, “Central blood pressure and hypertension: role in cardiovascular risk assessment,” *Clin. Sci.*, vol. 116, no. 4, pp. 273–282, Jan. 2009, doi: 10.1042/CS20080072.

[7] Y. Shi, P. Lawford, and R. Hose, “Review of Zero-D and 1-D Models of Blood Flow in the Cardiovascular System,” *Biomed. Eng. OnLine*, vol. 10, no. 1, p. 33, Apr. 2011, doi: 10.1186/1475-925X-10-33.

[8] M. R. Pfaller *et al.*, “Automated generation of 0D and 1D reduced-order models of patient-specific blood flow,” *Int. J. Numer. Methods Biomed. Eng.*, vol. 38, no. 10, p. e3639, 2022, doi: 10.1002/cnm.3639.

[9] H. Vogt, G. Atkinson, and P. Nenzi, “Ngspice User’s Manual Version 43plus (ngspice development version)”.

[10] P. H. Charlton, J. Mariscal Harana, S. Vennin, Y. Li, P. Chowienczyk, and J. Alastruey, “Modeling arterial pulse waves in healthy aging: a database for in silico evaluation of hemodynamics and pulse wave indexes,” *Am. J. Physiol.-Heart Circ. Physiol.*, vol. 317, no. 5, pp. H1062–H1085, Nov. 2019, doi: 10.1152/ajpheart.00218.2019.

[11] “Pulse Wave Analysis | IntechOpen.” Accessed: Aug. 28, 2024. [Online]. Available: https://www.intechopen.com/chapters/18367

[12] C. Montzka, V. R. N. Pauwels, H.-J. H. Franssen, X. Han, and H. Vereecken, “Multivariate and Multiscale Data Assimilation in Terrestrial Systems: A Review,” *Sensors*, vol. 12, no. 12, Art. no. 12, Dec. 2012, doi: 10.3390/s121216291.